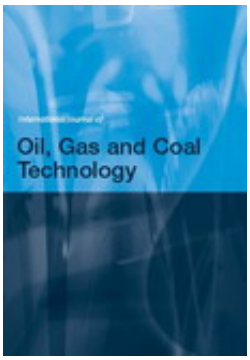
INDERSCIENCE PUBLISHERS
Linking academia, business and industry through research



International Journal of Oil, Gas and Coal Technology

ISSN online: 1753-3317 - ISSN print: 1753-3309
https://www.inderscience.com/ijogct

Influence of process parameters on conversion efficiency in plasma cracking of heavy oil residues

Artur Khakimov, Shuxratqodir Gulomov

DOI: 10.1504/IJOGCT.2026.10081578

Article History:

Received:	11 May 2025
Last revised:	01 February 2026
Accepted:	02 April 2026
Published online:	04 November 2026

Copyright © 2026 Inderscience Enterprises Ltd.

Influence of process parameters on conversion efficiency in plasma cracking of heavy oil residues

Artur Khakimov* and Shuxratqodir Gulomov

Tashkent Institute of Chemical Technology (TICT),
Navoi Avenue 32, Tashkent, Uzbekistan
Email: Khakimov.spd@gmail.com
Email: sh.gulomov@tkti.uz
*Corresponding author

Abstract: This study systematically investigates the influence of key process parameters – feedstock inlet temperature and flow rate – on the conversion efficiency and product distribution during the plasma cracking of heavy oil residues, with a focus on maximising the yield of the diesel fuel fraction (180–330°C). Experiments were conducted in a pilot-scale plasma reactor and it revealed that both parameters significantly affect diesel yield. An optimal feedstock temperature range of 200–350°C was identified, below which conversion is incomplete, and above which excessive gas formation occurs. Similarly, lower feedstock flow rates (0.5–0.75 dm^3/s) were found to enhance diesel yield by 30%–40% compared to higher rates (1 dm^3/s), which induce reactor instability and reduce cracking depth. The results provide a clear pathway for scaling plasma cracking technology as an energy-efficient and selective alternative to conventional methods for upgrading heavy residues into valuable middle distillates. [Received: June 3, 2025; Accepted: April 2, 2026]

Keywords: plasma cracking; heavy oil residues; diesel fuel; parametric study; process optimisation; conversion efficiency.

Reference to this paper should be made as follows: Khakimov, A. and Gulomov, S. (2026) 'Influence of process parameters on conversion efficiency in plasma cracking of heavy oil residues', *Int. J. Oil, Gas and Coal Technology*, Vol. 40, No. 5, pp.1–23.

Biographical notes: Artur Khakimov is a PhD candidate studying plasma chemical technologies applications for oil refining in the Tashkent Institute of Chemical Technology, Uzbekistan.

Shuxratqodir Gulomov is an Associate Professor at the Tashkent Institute of Chemical Technology, Uzbekistan with research interests in chemical engineering of oil and gas and catalysis.

In the oil industry, there are various methods for processing heavy and low-value raw materials into marketable products. In an oil refinery, light components are first extracted from crude oil. The remaining heavy fractions are then subjected to secondary conversion processes, such as cracking, to be chemically transformed into lighter, more valuable hydrocarbons with superior fuel properties. Cracking of petroleum hydrocarbons was originally carried out by thermal cracking, which has been almost completely replaced by catalytic cracking, as it yields a greater proportion of the gasoline fraction (IBP-180°C).

Copyright © The Author(s) 2026. Published by Inderscience Publishers Ltd. This is an Open Access Article distributed under the CC BY license. (http://creativecommons.org/licenses/by/4.0/)

Currently, the most commonly used process in oil refineries is fluid catalytic cracking (FCC) (Gary et al., 2007; Sadeghbeigi, 2012; Speight, 2010).

The feedstock for FCC is usually a fraction with an initial boiling point at atmospheric pressure of 340°C or higher and an average molecular weight in the range of almost 200 to 600. This fraction of oil is also called heavy gas oil. The FCC process vaporises and splits long-chain molecules of high-boiling hydrocarbon liquids into molecules with much shorter chains by contacting the feedstock, at high temperature and moderate pressure, with the so-called fluidised powder catalyst (Gary et al., 2007; Sadeghbeigi, 2012; Speight, 2010). In the FCC process, the reaction occurs at temperatures exceeding 510°C, utilising a finely fluidised catalyst. The process uses a reactor designed for the separation and regeneration of spent catalysts, which requires significant energy consumption and increases costs. Consequently, traditional cracking technologies must address challenges such as catalyst preheating time, the need for a hydrogen source, and coke removal (Speight, 2010). As an alternative technology that does not require the use of traditional catalysts, it is proposed to use non-thermal and/or low-temperature plasma technology, which has become widespread in the field of chemistry and materials processing (Fridman, 2008).

Conventional steam cracking and FCC operations face inherent limitations in heavy feedstock adaptability, including:

- high thermal energy requirements (Moulijn et al., 2013)
- rapid catalyst coking in heavy hydrocarbon environments (Bartholomew and Farrauto, 2006).

Sustained demand for light hydrocarbons, alongside significant disadvantages (e.g., high energy consumption, catalyst deactivation) associated with traditional conversion methods, necessitates the advancement of novel processing technologies for heavy oil residues.

Plasma technology has an ability to drive highly efficient non-equilibrium chemical processes. This makes it a promising candidate for applications such as cracking heavy oil residues (Bogaerts and Neyts, 2018).

Plasma cracking presents a disruptive alternative, utilising non-equilibrium plasma chemistry (Fridman and Kennedy, 2004) to achieve:

1 selective carbon-carbon (C-C) and carbon-hydrogen (C-H) bonds cleavage

2 reduced thermal cracking byproducts (methane, BTX)

3 improved feedstock flexibility without catalyst constraints (Riyanto et al., 2020).

The plasma cracking process involves several key steps:

- *Plasma initiation:* Plasma is generated by applying electrical energy to a gas in a reactor. This ionises the gas, producing a mixture of free electrons, ions and reactive particles.
- *Interaction with oil residues:* The oil residues are directly introduced into the plasma reactor, where they interact with the highly reactive plasma environment.
- *Formation of reactive particles:* The plasma generates reactive particles such as radicals, ions and excited molecules. These particles initiate and propagate chain reactions that fragment the large hydrocarbon molecules into smaller ones.

- *Cracking reactions:* The heavy hydrocarbons undergo cracking, a process where long-chain molecules are broken into shorter chains. This produces lighter hydrocarbons, such as methane, ethylene, and propylene, as well as hydrogen gas.
- *Products' stabilisation* for desired selectivity by removal of the initial (intermediate) products from plasma jet influence zone (also known as product quenching).
- *Product separation:* The cracked products are then separated into gases, liquid fuels, and non-reacted heavy oil residues. The gases can be used as feedstocks for petrochemical production, while the liquid fuels can be refined further.

The effectiveness of plasma cracking stems from the non-equilibrium nature of low-temperature plasma, where the energy distribution of reacting particles deviates from the Maxwell-Boltzmann equilibrium. Unlike conventional thermal processes, plasma-chemical reactions are governed by highly energetic electrons rather than bulk heating.

Plasma cracking technology can be implemented using various types of non-thermal and low-temperature plasma reactors. One of the simplest, inexpensive and frequently used reactors is dielectric barrier discharge reactor (DBDR) (Kogelschatz, 2003; Becker et al., 2005). This type of reactor is capable of generating plasma at atmospheric pressure and ambient temperature, which may be an advantage for industrial applications compared to traditional reactors used in thermo-catalytic processes. DBDRs are characterised by the presence of one or more insulating layers in the current path between the metal electrodes in addition to the discharge gap. Applying high voltage between the two electrodes creates an ionised space with electrons with high initial energy, both internal (degree of ionisation) and external (kinetic) energy. When hydrocarbons are fed into a reactor with ionised matter, excited electrons collide with hydrocarbon molecules, and if there is enough energy during the collision of these particles, the C-C and C-H bonds are broken. In a plasma environment, active particles such as electrons, ions, and excited particles (radicals, ions) can simultaneously act as energy carriers and catalytic agents. Collisions of electrons and ions with heavy hydrocarbons form activated radicals, which in turn recombine and lead to the production of hydrocarbons with shorter chains – the desired products of the process. Although the complex plasma-hydrocarbon interactions are not fully understood, this approach can yield products with a higher olefin content, making them more valuable than those from thermal cracking.

It is well known that cold plasma has low energy consumption and easily shifts thermodynamic equilibrium, due to which the desired chemical selectivity of reactions is achieved (Neyts et al., 2015). The chemistry of processes in such systems is determined precisely by the high energy of electrons, which also helps to achieve the desired chemical selectivity of the process.

The key advantage of plasma cracking is achieved through the following features:

- High electrons' 'energy' (30,000–100,000 K in thermal units), enabling efficient band cleavage without requiring extreme bulk gas temperatures.
- Selective energy deposition, where electrons transfer energy directly to chemical bonds, minimising thermal losses.
- Ambient heavy-particle temperatures, allowing reactions to proceed without excessive heat input.

Plasma cracking offers further advantages: it operates without high overpressure, eliminating the need for capital-intensive equipment such as massive hydrocracking reactors, separate hydrogen production units, or process catalysts.

A number of published studies also show that C1–C9 hydrocarbon molecules are successfully cracked by various types of non-thermal plasma reactors. In addition, such reactions can lead to the formation of hydrocarbons and oxygen-containing compounds heavier than the feedstock, which occurs due to the combination of radicals in cold plasma reactors (Khani et al., 2011; Prieto et al., 2008; Holladay et al., 2009; Jahanmiri et al., 2012; Khademi et al., 2009; Bibikov et al., 2007; Slovetskii, 2006; Suttikul et al., 2012; Pierce et al., 2009; Nomura et al., 2009; Malik et al., 2013).

For example, Khani et al. (2014) described an experimental setup for studying the possibility and proving the ability of cold plasma to split heavy hydrocarbons (n-hexadecane, lubricating oil and heavy oil) into lighter hydrocarbons.

A number of studies demonstrate the advantages of using electric arc (non-thermal) plasma for heavy hydrocarbon decomposition (Zalyaletdinov, 2011; Yarullin, 2000; Ganieva et al., 2015, 2011; Lemont et al., 2018).

Thus, the electrical characteristics of the reactor and its power consumption are directly related to the electron energy distribution of the ionised medium. Therefore, during the tests, the plasmatron was operated at its constant maximum power setting to achieve and maintain the highest ionisation energy. Most scientific papers devoted to studying the dependence of plasma properties on energy consumption use the Lissajous method (Holub, 2012).

There are two possible mechanisms: hydrocarbon cracking and hydrocarbon activation (creation of more reactive species). The former is based on electron-mediated processes such as dissociation, dissociative ionisation, vibrational excitation, and electron excitation of the parent hydrocarbon molecule, resulting in the formation of parent hydrocarbon fragments, radicals, or excited species (ions, ion-radicals).

The second mechanism is ion-molecular reactions, in which ions created by collisions with electrons (bombardment) react with neutral gas particles and produce particles that can stimulate reactions.

The non-thermal plasma environment enables unique reaction pathways:

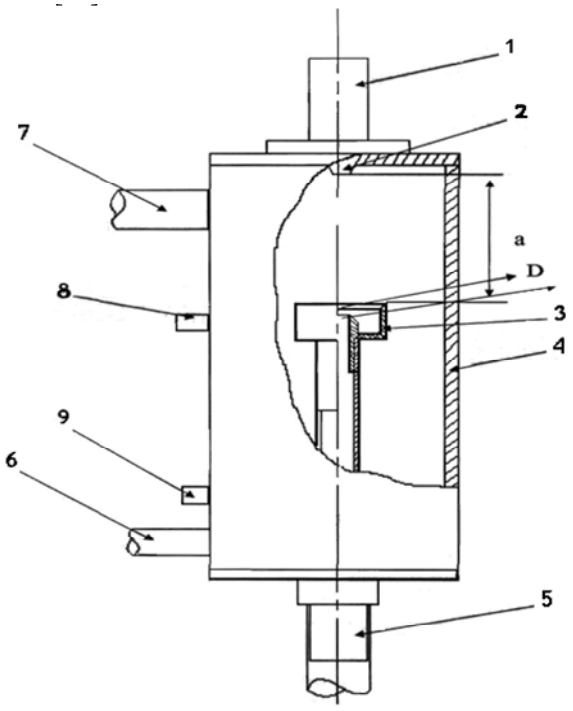
- *electron-impact dissociation* ($e^- + RH \rightarrow R\bullet + H\bullet + e^-$)
- *radical-driven propagation* ($R\bullet \rightarrow$ Olefin + smaller radical)
- minimal thermal oligomerisation side reactions.

As a result of ionic recombination and/or charge transfer reactions following dissociative ionisation, smaller, more flammable molecular fragments are formed.

In Khakimov et al. (2012), the authors describe a plasma cracking unit that utilises a jet of low-temperature plasma. Unlike typical cold plasma systems, this jet configuration delivers higher initial energy and creates an elevated temperature in the reaction zone. This reduces the required plasma exposure time and enhances selectivity towards the desired target products. An important fact is that the experiments were carried out on an industrial unit in which the feed (raw material) already possessed significant initial velocity and energy (temperature up to 350–360°C), as well as a small excess pressure.

The authors implemented a 20-litre (dm^3) custom reactor in an oil refining setup, achieving up to 95% conversion of the feedstock into valuable gasoline and diesel components. The energy consumption was at least three times lower ($5.99 \cdot 10^5$ kJ per ton) compared to traditional catalytic cracking ($14.46 \cdot 10^5$ kJ per ton).

Figure 1 Device for plasma-chemical processing of heavy hydrocarbon fractions



Note: 1 – plasma torch, 2 – plasma torch nozzle, 3 – heavy fraction feed nozzle, 4 – reactor, 5 – heavy fraction feed, 6 – outlet of unreacted portion of heavy fractions (recirculate), 7 – product outlet into rectification column, 8 – outlet temperature sensor and 9 – inlet level sensor.

In the present work, we propose a plasma-chemical processing unit for converting heavy hydrocarbon fractions into light petroleum products. Fuel oil feedstock preparation and product fractionation can be performed using standard refinery equipment. The core processing device (Figure 1) features an adjustable distance between the plasma torch nozzle and the reactor body. This design provides several technical and economic advantages over conventional hydrocarbon processing methods. Furthermore, the installation is constructed using commercially available components, including the plasma power source, torch and compressor.

To apply the plasma torch to the hydrocarbons we propose the reactor, which schematically depicted on Figure 1 (Belichenko et al., 2008).

Figure 3 is a real picture of a low temperature plasma cracking reactor with dismantled plasmatron.

Figure 2 Plasma torch illustration (see online version for colours)

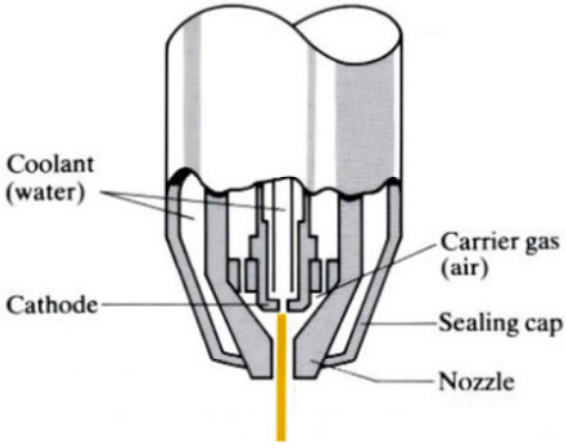


Figure 3 Photo of the actual plasma cracking reactor used for current research (see online version for colours)



The main technical characteristics of the reactor provided in Table 1.

The plasma torch producer – plasmatron is designed for air-flame cutting of ferrous and non-ferrous metals, and can be used to supply plasma to the reactor for plasma-chemical processing of heavy hydrocarbon fractions.

For the experiments the standard metal-cutting PURM-400VA plasma torch was used.

The plasma torch is a device for creating and stabilising a compressed electric arc burning between the cathode and anode electrodes in a flaw of plasma-forming and stabilising gas.

The degree of ionisation of the plasma used in plasma cutting machines such as the PURM 400VA is approximately 10^{-3} to 10^{-2}, which means that the plasma belongs to the category of weakly ionised gases. This is typical for plasma streams used in air plasma cutting (operating current of 70–350 A, plasma arc temperature of approximately 10,000–30,000 K), where the electron concentration remains at the level of thousandths

of a fraction compared to neutral particles (Purm.ru, https://purm.ru/product/apparat-plazmennoj-rezki-metalla-purm-400va/).

Table 1 Plasma cracking reactor technical parameters

Parameter	*Value/specification*
Maximum power input	60 kW
Design feedstock capacity	50 metric tons/day
Operating temperature range	
Minimum	Not limited
Maximum	500°C
Maximum operating pressure	0.5 MPa
Dimensions (H × D)	0.6 m × 0.2 m
Weight	8.2 kg

The main units and parts of the plasma torch are: an electrode holder with a deflector, an insulating housing, a housing fastening nut, a housing, a mouthpiece, an electrode and a nozzle.

The plasma torch operates as follows: cooling water and plasma-forming gas are fed into the plasma torch. The open-circuit voltage of the device's power source is fed to the cathode and anode. The pen-circuit voltage is fed to the electrode and nozzle through the pilot arc circuit so that the nozzle is at a positive potential. When the pen-circuit voltage of the power source is applied, periodically repeating current pulses are excited between the electrode and the nozzle using the arc exciter, which create a visible pilot arc torch. The main arc is excited automatically when the visible pilot arc torch touches the surface of the 'mass'. After the current reaches the set value, the process proceeds stably within the range of current and voltage in the arc provided by the power source. Water vapour under pressure is fed into the channel in the insulating housing, then through the cavity between the electrode holder and the insulating housing it enters the cavity between the cathode and the nozzle and is blown out through the nozzle channel.

High voltage is supplied through the pilot arc current lead to the housing and then to the nozzle (anode). The operating voltage is supplied to the electrode holder and then to the electrode (cathode).

The unit can use both direct and indirect plasma torches.

The plasma-forming medium is air.

The determining dimensions of the nozzle are the outer diameter D and the diameter of the outlet opening d.

The outer diameter D of the nozzle is equal to the diameter of the plasma spot at the lower limit of the distance a.

The diameter of the outlet opening d is selected based in the condition of equality to the diameter of the plasma spot at the upper limit of the distance a, i.e., at the maximum approach of the nozzle to the nozzle.

The distance a from nozzle 2 to nozzle 3 is set depending on the device operating mode, the power of the plasma unit and is limited by the limits:

- the lower limit is a plane perpendicular to the plasma beam with a plasma temperature of 300°C

- the upper limit is determined by the design of the nozzle.

Before starting work, air oxygen is removed from the reactor by blowing it with water vapour or inert gas.

After the plasma torch 1 initiation plasma exuding nozzle is placed to initial position at a distance of 25–30 mm from the nozzle, raw material (heavy feedstock) is supplied toward the plasma, cracking process starts in a contact point. The products of reactions – light hydrocarbon cuts are obtained at the outlet 7 as mixture of a gaseous and droplets of heavy hydrocarbon cuts entrained by stream to the fractioning column. The residuum cut (> 350°C) is returned through the outlet 6 for recirculation.

The percentage content of a particular oil product in the mixture is regulated by changing the distance *a*. Thus, with an increase in the distance *a*, the content of gasoline cut in the mixture increases, and with a decrease, the content of diesel fuel components increases.

Table 2 Effect of feed temperature on the fractional composition of plasma cracking process products

Average boiling point of the products t, °C					
Fraction yield, %	*Feedstock inlet temperature to the reactor*				
	100°C	*120°C*	*200°C*	*300°C*	*350°C*
5	203	198	165	176.1	178.3
10	259	215	180	191.8	193
20	307	260	188.7	204.9	206.4
30	-	335	207	215	218
40	-	-	224	225.3	227.5
50	-	-	239.1	234.6	240.2
60	-	-	255	248.3	252.1
70	-	-	271.9	261	268
80	-	-	294.7	274.7	281.2
90	-	-	300.8	294.8	298.8
95	-	-	-	320	313
Residue, %	73	68	10	5	3
Product boiling point	49	52	84.5	40	62
Product final boiling point	350	350	349.5	334.2	347.2

During the experiments, it was possible to empirically identify the dependences of the fractional composition of the process products on the feed rate, the initial temperature of the raw material and other process parameters. The dependence of the composition of the process products on the initial temperature of the raw material supplied to the reactor is shown in Table 2.

Experiments show that the optimal for feedstock temperature range is 200°C to 350°C. With the temperature less than 200°C, the initial substance energy is not enough for productive cracking processing.

To evaluate the effect of varying the feedstock feed rate (0.5 to 1 dm^3/s) into the reaction zone, the system was operated at a constant feedstock inlet temperature of 300°C to ensure process stability.

Table 3 presents the relationship between the fractional composition of plasma cracking process products and the feedstock feed rate.

Table 3 Dependence of plasma cracking process products fractional composition on feedstock feed rate to the reactor

Recovery rate, %	*Average boiling point of the products, °C*		
	Raw material throughput, dm^3/s		
	0.5	*0.75*	*1*
5	154	176	189
10	173	192	217
20	199	205	236
30	218	215	259
40	243	225	274
50	286	234	283
60	312	248	340
70	345	261	
80		275	
90		295	
95		320	
Residue, %	4	5	34
Product boiling point	40	40	80
Product final boiling point	330	334	350

It was found out experimentally that in case of too low flow rate, raw materials often pass the stage of the target highly profitable product – a component of liquid motor fuel (gasoline, kerosene/jet fuel, diesel fuel), decomposing to hydrocarbon gases. In case of high flow rate through the above-described reactor, the degree of raw material conversion decreases sharply.

Increasing the feed rate beyond 1 dm^3/s raises reactor pressure, resulting in plasma torch instability and reaction termination.

To determine the combined effect of the feedstock feed temperature (straight distillation residue > 350°C) and its feed rate into the reactor, the method of mathematical experiment planning was used according to the scheme of a full factorial experiment (Table 4).

This planning allowed us to take into account the simultaneous change of all factors influencing the process, which made it possible to establish the degree of their interaction, significantly reduce the number of experiments and obtain the necessary data for designing or selecting an industrial apparatus.

Given market-driven constraints and an inability of IBP-180°C cut to satisfy current automotive gasoline standards, the process was reconfigured to yield a diesel fuel component (the 180–330°C cut) as its primary product.

Table 4 Full factorial experiment FFE 2^2 in plasma cracking process products of the residue

Optimisation factors and parameters	*Feedstock inlet temperature, °C*	*Flow rate, V, dm³/s*
Code	X_1	X_2
Base level (0)	200	0.75
Variation interval (ΔX)	100	0.25
Upper level (+1)	300	1.0
Lower level (–1)	100	0.5

Note: Where X_j = natural value of the factor, X_{j0} = natural value of the factor's base level, and ΔX_j = variation interval of the j^{th} factor.

The key process parameters selected as the main variable factors affecting plasma cracking process products were:

- feedstock inlet temperature (X_1): 100–300°C
- reaction zone flow rate (X_2): 0.25–1 dm³/s.

Process efficiency was assessed by the diesel fraction yield (Y). Analyses were conducted in triplicate. The required number of experiments (N) was determined by the following formula:

$$N = n^k$$

where

n number of levels

k number of factors.

For any factor Z_j:

$$Z_j^0 = \frac{Z_j^{\max} + Z_j^{\min}}{2},\ j = 1, 2, \ldots, k$$

$$\Delta Zj = \frac{Z_j^{\max} - Z_j^{\min^0}}{2}.$$

The point with coordinates $(Z_1^0, \ldots, Z_k^0)$ represents the design centre, ΔZj while denotes the variation interval along the axis Zj. Through linear transformation of variables Z_1, …, Z_k, we obtain coded variables X_1, …, X_k:

$$Xj = \frac{Zj - Z_j^0}{\Delta Zj};\ j = 1, 2, \ldots, k.$$

The coded variables X_1, …, X_k have: upper level: +1, lower level: –1 and centre point: 0.

Experiments planning matrix with dummy variable ($X_0 = 1$) is presented in Table 5.

To obtain the regression equation, the results were mathematically processed.

The homogeneity of variances $S_j^2,\ j = 1, 2, \ldots, N,$ was checked using the Cochran criterion.

Table 5 Extended second-order design matrix (FFD2²)

Exp.#	X_0	X_1	X_2	$X_1 X_2$	Y	S^2
1	+1	–1	–1	+1	Y_1	$S^2 1$
2	+1	+1	–1	–1	Y_2	$S^2 2$
3	+1	–1	+1	–1	Y_3	$S^2 3$
4	+1	+1	+1	+1	Y_4	$S^2 4$

Calculated value of the Cochran criterion:

$$G_{\max} = \frac{S^2_{i\max}}{\sum_{i=1}^{N} S_i^2}$$

Table value of the Cochran criterion G_{cr}, at a significance level of $p = 0.05$ with degrees of freedom: $\nu_1 = m - 1 = 2$; $\nu_2 = N = 4$, where m is the number of duplicate experiments, $m = 3$; N is the number of experiments in the plan, with $n = 2$ and $k = 2$ the number of possible combinations $N = 4$.

When conducting the studies, special attention was paid to the reproducibility of the experiments. The dispersion was considered homogeneous, and therefore, the experiments were reproducible if the following condition was met:

$$G_{\max} \left\langle G_{кр} \left(\nu_1, \nu_2\right)\right.$$

Then the disquisition of variance of the experimental error to represented as:

$$S^2_{err} = \frac{1}{N}\sum_{i=1}^{N} S_i^2$$

Next, the coefficients of the selected model were calculated.

The dispersion of the coefficients ($S^2\{bj\}$) was estimated with the number of degrees of freedom:

$$\nu_b = N(m-1); \qquad S^2\{bj\} = \frac{S^2_{ош}}{Nm}.$$

The standard deviation of the coefficient estimates was determined: $S\{bj\}$. Then, the significance of the coefficients was estimated using the Student criterion. After excluding insignificant coefficients, an equation with significant coefficients written. The second-order regression equation obtained on the basis of the experimental data was written as follows:

$$\hat{Y} = b_0 + b_1 X_1 + b_2 X_2 + b_{12} X_1 X_2$$

where

b_0 is the free term of the regression equation

b_1 and b_2 are linear effects

b_{12} is the effect of pairwise interaction.

Then, the adequacy of the obtained model to the experiment was verified using Fisher's criterion.

Estimation of residual variance:

$$S_{res}^2 = \frac{m}{N-d}\sum_{i=1}^{N}\left(\overline{y}_i - \hat{y}_i\right)^2$$

where d is the number of significant coefficients in the regression equation.

Calculated value of the F-ratio:

$$F = \frac{S_{res}^2}{S_{err}^2}$$

Tabular value of F_{cr} – ratio for the corresponding degrees of freedom: numerator – $\nu_{res} = N - d$, denominator – $\nu_{err} = N(m-1)$.

The resulting model adequately represented the results of the experiment if the condition was met $F \langle F_{cr}$. Otherwise, additional experiments were conducted.

As a result of mathematical processing of the actual results of experiments on the combined effect of temperature and feed rate into the reactor on the process of plasma cracking of heavy residues, the following regression equation was obtained:

$$Y = 40.1 + 9.7X_1 - 3.9X_2 + 4.2X_1X_2$$

where

Y is the yield of the diesel fraction during plasma cracking process

X_1 is the feed temperature into the reactor

X_2 is the feed rate into the reactor.

The following conclusions can be made from the analysis of the coefficients of the regression equation: an increase in the feed temperature into the reactor increases the yield of the diesel fraction (the coefficient at X_1 is positive). An increase in the feed rate of the feed into the reactor in the studied range reduces the yield of the diesel fraction (the coefficient at X_2 is negative). The influence of the coefficient of pairwise interaction of temperature and feed rate increases the treatment effect. It also follows from the analysis of the equation that the positive effect of increasing the temperature is more than two times higher than the negative effect of the feedstock feed rate in the selected intervals of factor variation. While beneficial for conversion, increasing the feedstock preheat temperature is economically and operationally constrained by higher energy costs and the risk of feed-line fouling due to premature thermal cracking. For these reasons, the experimental analysis focused on two representative inlet temperatures: 200°C and 300°C.

The results were analysed, establishing the dependence of the plasma cracking product distribution on the feedstock inlet temperature. Gas chromatographic analysis was conducted on an Agilent 6890 N system fitted with a flame ionisation detector (FID) to determine the composition of both feedstock and products. The ChemStation data system was used for instrument control and data processing. The chemically cross-linked stationary phase of RTX-1 is non-polar.

In this work, an RTX-1 capillary column measuring 30 m in length and 0.25 mm in internal diameter was used.

Figure 4 Chromatogram of the raw materials of the process (see online version for colours)

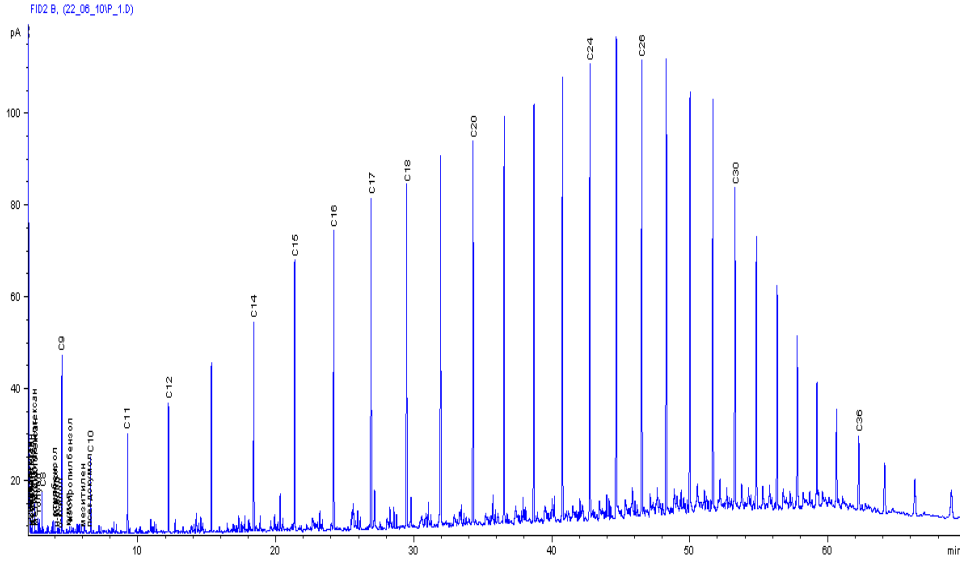


Figure 5 Chromatogram of the product of the process with a feed temperature of 200°C (see online version for colours)

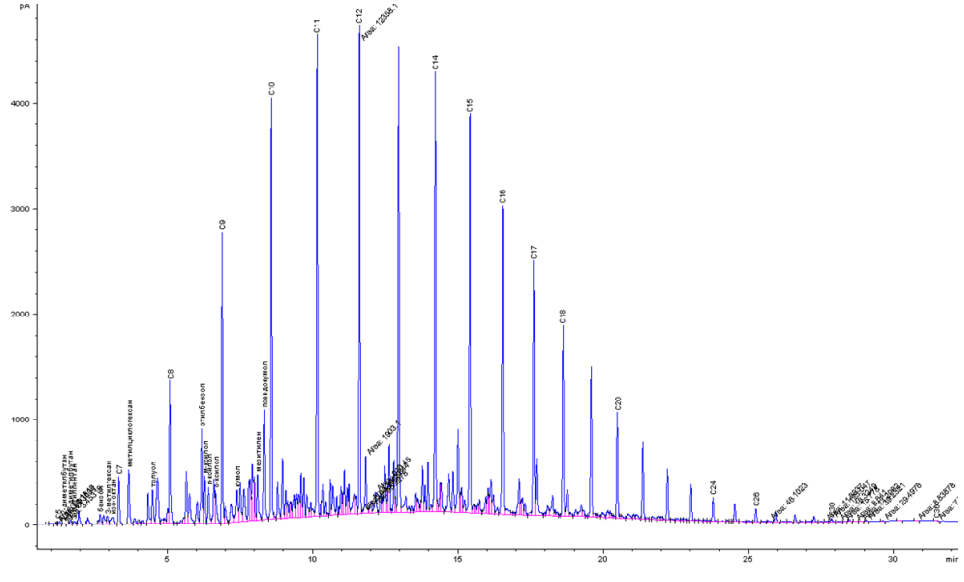
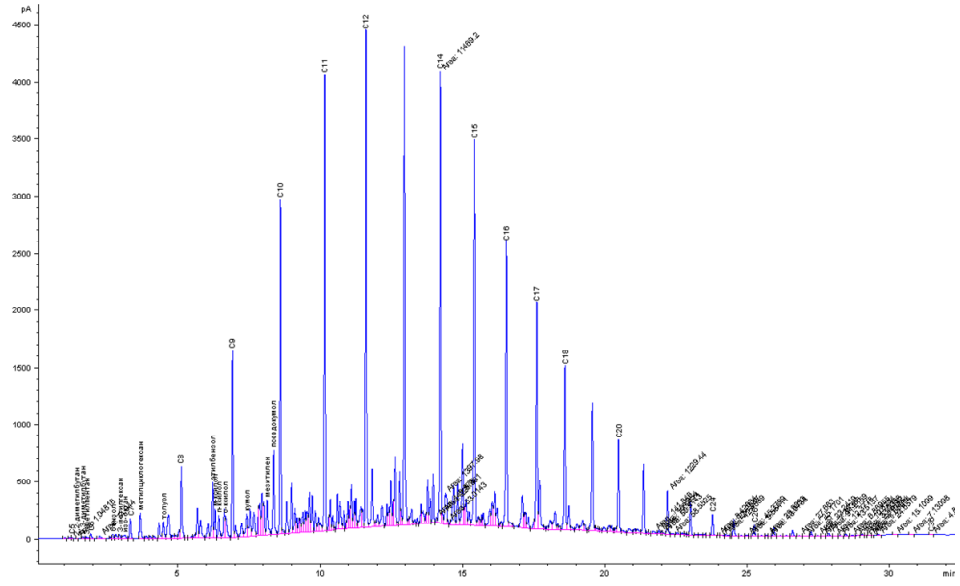
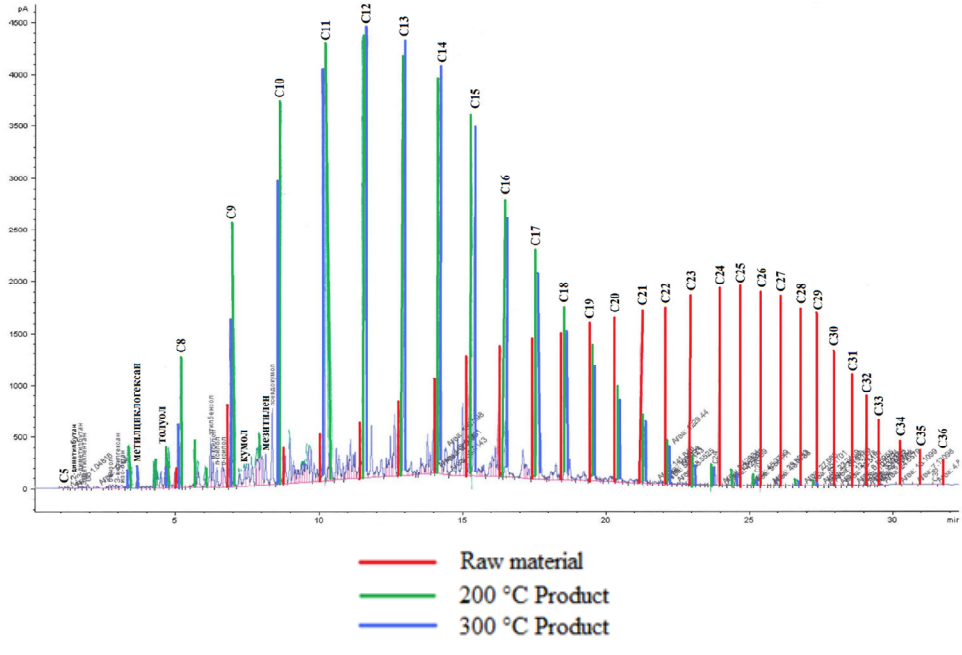


Figure 6 Chromatogram of the product of the process with a feed temperature of 300°C (see online version for colours)



For comparison, Figure 7 presents the superposition of chromatograms of the raw material and products of the plasma cracking process obtained with a feed temperature of 200°C and 300°C.

Figure 7 Superimposition of chromatograms of the raw material and products of the plasma cracking process (see online version for colours)



The plasma cracking of feedstocks (fuel oil) exhibited negligible coke formation, a notable result given the extreme local temperatures (~30,000°C at the burner outlet) in the feedstock-plasma contact zone and the known coking propensity of petroleum feedstocks under cracking conditions. No coke was detected in the process products. Furthermore, the reactor's internal surfaces, including the electrodes, were not cleaned during the entire experimental series. As evidenced by the photograph below of the receiving electrode and feedstock injection nozzle (the direct plasma contact points), only insignificant traces of coke are present.

Figure 8 Photograph of the reaction chamber of the plasma cracking reactor (see online version for colours)



The pilot reactor maintained stable operation, producing the target product in continuous runs averaging 36 hours. Consequently, electrode coking is not a factor influencing the operational stability of this process. However, due to the inherent nature of the plasma process and the associated electrodes erosion, the electrodes are classified as consumable components. Their replacement schedule will be determined by a maintenance strategy that combines condition-based monitoring and a time-based approach, to be refined during further pilot-scale operation.

The proposed mechanism for plasma-catalytic upgrading of heavy residues in a steam environment involves several concurrent stages. Upon injection into the steam plasma jet, the feedstock is subjected to a flux of highly reactive species – including electrons, ions (H^+, O^+, OH^+), radicals (H•, O•, OH•), and excited molecules – generated by the dissociation and ionisation of H_2O in the electric arc. This reactive medium initiates radical-chain cracking of high-molecular-weight hydrocarbons, leading to their fragmentation.

The resulting unsaturated fragments (olefins, alkynes) subsequently undergo hydrogenation and isomerisation. These reactions are catalysed in situ by the tungsten-based electrodes, whose surface, under process conditions, consists of active tungsten oxides and sulphides known for their hydrogenation and isomerisation functionality.

Concurrently, organic sulphur compounds (e.g., thiophenes, sulphides) are transformed via two primary pathways:

1 reductive hydrodesulphurisation (HDS) to form H_2S and the corresponding hydrocarbon

2 partial oxidation to yield disulphides, sulfoxides, and sulfones, which are predominantly concentrated in the heavier or polar fraction.

The dominance of the reductive or oxidative route is determined by the local redox potential in the plasma zone, governed by the H_2O/H_2 ratio.

Schematically, this can be represented as follows:

1 The chain's initiation:

a $H_2O \rightarrow H + H + O + Q$ (460 kJ/mol)

b $CH_3-(CH_2)_{13}-CH_2-CH_3 \xrightarrow{t,\vec{e},h\upsilon} CH_3-(CH_3)_{13}-CH_2^{\bullet}+CH_3^{\bullet}$

Collisions between hydrocarbon molecules cause outer $^{\bullet}H$ ejection

c $CH_3-(CH_2)_{14}-CH_2\int H \leftrightarrow CH_3-(CH_2)_{14}-CH_2^{\bullet}+{}^{\bullet}H.$

2 Chain continuation:

a $CH_3-(CH_2)_{14}-CH_3+H^{\bullet} \rightarrow H_2+CH_3-(CH_2)_{14}-CH_2^{\bullet}$

Radical decomposition via β-bond cleavage (C-C и C-H)

$$CH_3-(CH_2)_n-CH^{\bullet}-CH_2\int CH_3 \leftrightarrow \left[CH_3-(CH_2)_n-CH^{\bullet}-CH_2^{\bullet}\right]+{}^{\bullet}CH_3$$

b

$$\downarrow$$

$$CH_3-(CH_2)_n-CH=CH_2$$

$$H^{\bullet}$$

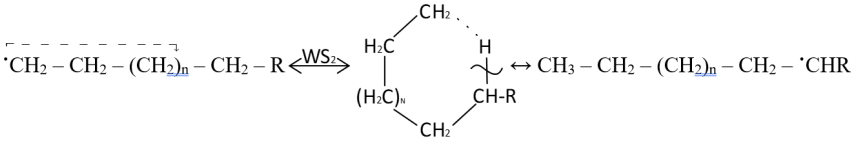
$$|$$

c $$CH_3-(CH_2)_n-CH^{\bullet}-CH^{\bullet}-CH_3 \leftrightarrow \left[CH_3-(CH_2)_n-CH^{\bullet}-CH^{\bullet}-CH_3\right]+{}^{\bullet}H$$

$$\downarrow$$

$$CH_3-(CH_2)_n-CH=CH-CH_3$$

$E_{diss.}$ = 42–84 kJ/mol.



If $CH_3-(CH_2)_n-CH_2^-$ is R, then

$R\text{-}H + H^{\bullet} \leftrightarrow H_2 + {}^{\bullet}R$

$R\text{-}H + {}^{\bullet}CH_3 \leftrightarrow CH_4 + {}^{\bullet}R$

$R\text{-}H + {}^{\bullet}C_2H_5 \leftrightarrow C_2H_6 + {}^{\bullet}R,$

etc.

c Chain termination:

$${}^{\bullet}CH_3 + {}^{\bullet}CH_3 \leftrightarrow CH_3-CH_3$$

$$^{\bullet}CH_3 + {}^{\bullet}CH_3 \leftrightarrow CH_3 - CH_3$$

$$CH_3 - CH_2 - {}^{\bullet}CH_2 + {}^{\bullet}CH_3 \leftrightarrow CH_4 + CH_3 - CH = CH_2$$

4 Hydrogenation:

$$CH_3 - CH = CH_2 + 2H^{\bullet} \xrightarrow{WO_3} CH_3 - CH_2 - CH_3$$

$$CH_3 - CH = CH_2 - (CH_2)_n - CH_3 \xrightarrow{WO_3} CH_3 - CH_2 - CH_2 - (CH_2)_n - CH_3,$$

при $n > 13$.

The unsaturated hydrocarbons produced by thermal cracking are hydrogenated to form saturated paraffins. Additionally, partial hydrogenation and hydrocracking of polycyclic aromatic and resin-asphaltene constituents may occur. Concurrently, organosulphur compounds undergo hydrogenolysis. For example, mercaptans are converted to hydrogen sulphide and the corresponding hydrocarbons:

$$RSH + H_2 \rightarrow RH + H_2S$$

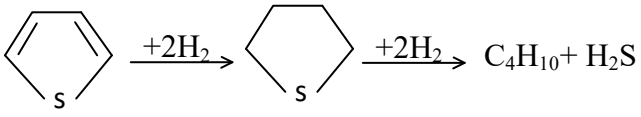
Sulphides undergo hydrogenation via mercaptan intermediate formation:

$$RSR^{\bullet} + H_2 \rightarrow RSH + R^{\bullet}H \xrightarrow{+H_2} RH + R^{\bullet}H + H_2S$$

Disulphides undergo hydrogenation via an analogous mechanism:

$$RSSR^{\bullet} + H_2 \rightarrow RSH + R^{\bullet}SH \xrightarrow{+H_2} RH + R^{\bullet}H + 2H_2S$$

Cyclic sulphides (e.g., thiophene and thiophane) are hydrogenated to form corresponding aliphatic hydrocarbons:



Benzothiophenes and dibenzothiophenes undergo hydrogenation via the following scheme (Ryabov, 2004):

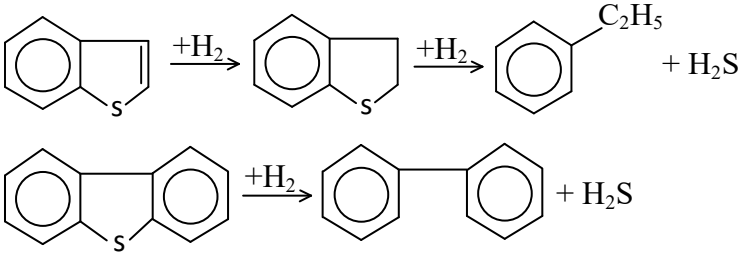


Table 6 represents the change in the component composition of the plasma cracking process raw material (fuel oil) and products of the plasma cracking process obtained with a feed temperature of 200°C and 300°C.

Table 6 Peak table of hydrocarbon content in the initial feedstock and products of plasma cracking

Hydrocarbon	*The feedstock is the still residue from the atmospheric distillation column*	*Plasma cracking product with feed temperature to the reactor*	
		200°C	*300°C*
	Content in petroleum product, %		
n-Butane (C_4)		0.011	0.017
Isobutane (iC_4)		0.021	0.02
n-Pentane (C_5)	0.013	0.04	0.022
Isopentane (iC_5)		0.024	
n-Hexane (C_6)		0.206	0.078
Isohexane (iC_6)	0.193	0.141	0.127
n-Heptane (C_7)	0.057	0.64	0.297
Isoheptane (iC_7)	0.125	1.327	0.209
Methylcyclohexane	0.01	0.867	0.447
n-Octane (C_8)	0.122	1.862	1.072
Isooctane (iC_8)	0.255	2.341	1.297
n-Nonane (C_9)	0.623	3.199	2.36
Isononane (iC_9)	0.065	2.575	1.71
n-Decane (C_{10})	0.342	4.596	4.213
Isodecane (iC_{10})	0.419	4.413	3.622
n-Undecane (C_{11})	0.542	5.567	5.007
Isoundecane (iC_{11})	0.57	5.307	5.238
n-Dodecane (C_{12})	0.729	5.452	4.993
Isododecane (iC_{12})	0.763	4.486	6.296
n-Tridecane (C_{13})	1.027	5.649	6.698
Isotridecane (iC_{13})	0.972	4.484	5.281
n-Tetradecane (C_{14})	1.362	5.391	6.251
Isotetradecane (iC_{14})	1.191	2.881	2.978
n-Pentadecane (C_{15})	1.76	4.823	5.592
Isopentadecane (iC_{15})	1.434	4.126	4.784
n-Hexadecane (C_{16})	2.01	3.042	2.41
Isohexadecane (iC_{16})	1.142	2.313	4.338
n-Heptadecane (C_{17})	2.297	3.176	3.504
Isoheptadecane (iC_{17})	1.089	1.561	1.574
n-Octadecane (C_{18})	2.403	2.412	2.656
Isooctadecane (iC_{18})	1.4	1.732	1.828
n-Nonadecane (C_{19})	2.647	2.006	2.142
Isononadecane (iC_{19})	1.487	1.017	1.001
n-Eicosane (C_{20})	2.794	1.387	1.432
Isoeicosane (iC_{20})	1.43	0.597	0.585

Table 6 Peak table of hydrocarbon content in the initial feedstock and products of plasma cracking (continued)

Hydrocarbon	*The feedstock is the still residue from the atmospheric distillation column*	*Plasma cracking product with feed temperature to the reactor*	
		200°C	*300°C*
	Content in petroleum product, %		
n-Heneicosane (C_{21})	2.98	1.008	1.049
Isoheneicosane (iC_{21})	1.359	0.416	0.392
n-Docosane (C_{22})	3.11	0.687	0.689
Isodocosane (iC_{22})	1.491	0.275	0.251
n-Tricosane (C_{23})	3.406	0.508	0.502
Isotricosane (iC_{23})	1.536	0.189	0.17
n-Tetracosane (C_{24})	3.419	0.248	0.342
Isotetracosane (iC_{24})	1.517	0.112	0.09
n-Pentacosane (C_{25})	3.738	0.284	0.271
Isopentacosane (iC_{25})	1.379	0.073	0.057
n-Hexacosane (C_{26})	3.653	0.216	0.207
Isohexacosane (iC_{26})	1.812	0.072	0.059
n-Heptacosane (C_{27})	3.668	0.178	0.166
Isoheptacosane (iC_{27})	1.835	0.059	0.057
n-Octacosane (C_{28})	3.414	0.129	0.117
Isooctacosane (iC_{28})	1.777	0.064	0.057
n-Nonacosane (C_{29})	3.365	0.107	0.092
Isononacosane (iC_{29})	1.936	0.057	0.042
n-Triacontane (C_{30})	2.821	0.077	0.063
Isotriacontane (iC_{30})	1.812	0.039	0.03
n-Hentriacontane (C_{31})	2.416	0.054	0.045
Isohentriacontane (iC_{31})	1.69	0.037	0.027
n-Dotriacontane (C_{32})	1.867	0.04	0.031
Isodotriacontane (iC_{32})	1.423	0.028	0.023
n-Tritriacontane (C_{33})	1.528	0.036	0.027
Isotritriacontane (iC_{33})	1.233		0.017
n-Tetratriacontane (C_{34})	1.174	0.031	0.021
Isotetratriacontane (iC_{34})	0.894		
n-Pentatriacontane (C_{35})	0.995	0.026	0.016
Isopentatriacontane (iC_{35})	1.013		
n-Hexatriacontane (C_{36})	0.861	0.025	
Isohexatriacontane (iC_{36})	0.817		0.016
n-Heptatriacontane (C_{37})	0.696		
Isoheptatriacontane (iC_{37})	0.635		
n-Octatriacontane (C_{38})	0.613		

Table 6 Peak table of hydrocarbon content in the initial feedstock and products of plasma cracking (continued)

Hydrocarbon	*The feedstock is the still residue from the atmospheric distillation column*	*Plasma cracking product with feed temperature to the reactor*	
		200°C	*300°C*
	Content in petroleum product, %		
Isooctatriacontane (iC_{38})	0.066		
n-Nonatriacontane (C_{39})	0.538		
Isononatriacontane (iC_{39})	2.416	0.054	0.045
Benzene		0.172	0.082
Toluene	0.024	0.565	0.299
Ethylbenzene	0.059	1.347	0.908
m-Xylene	0.045	0.63	0.426
p-Xylene	0.014	0.576	0.398
o-Xylene	0.011	0.632	0.472
Cumene	0.021	0.618	0.48
Pseudocumene	0.014		1.275
Isopropylbenzene	0.041		
1,3,5-Trimethylbenzene	0.011	0.608	
1,2,4-Trimethylbenzene		0.105	
Mesitylene			0.655
Total	100	100	100

The data presented in Table 6 focuses exclusively on the hydrocarbon composition. All non-hydrocarbon components and impurities were excluded from the final analysis, and the results were normalised to 100%.

As can be seen from the data provided, as a result of treating fuel oil with an ionisation medium, high-molecular compounds quantity, starting with C18, including hydrocarbons of normal structure, are decreasing in the products. Unsaturated hydrocarbons (up to 5% mass.) are present in the products, but normal hydrocarbons predominate. The ratio of n-alkanes to iso-alkanes is approximately 3:1. The content of light aromatic compounds in plasma chemical treatment products increases significantly compared to raw materials.

From the analysis of the chromatographic study data, it follows that the product obtained at a feedstock feed temperature of 300°C has a narrower component composition. This means that from the point of view of obtaining target products – blending component for diesel fuel, the process is more efficient than the process occurring at a feedstock feed temperature of 200°C.

The authors of this article see the potential of using methane as a plasma-forming gas or introducing methane into a plasma stream of another ionised gas for the purpose of its subsequent plasmolysis and enrichment with hydrogen. Its radicals and ion radicals of the primary contact zones, reaction and quenching of the raw material of the plasma cracking process of heavy oil residues of the primary distillation of oil as a further development of plasma cracking technology and a promising direction of research.

Vodopyanov et al. (2022), Taghvaei et al. (2013) and Bromberg et al. (1998) describe methods for obtaining hydrogen by plasma cracking. For example, the work describes the process of pyrolysis (plasmolysis) of methane using a high-frequency induction plasma torch of atmospheric pressure, similar in design and method of ionisation of the plasma-forming gas to the technology of plasma cracking of heavy oil residues studied by the authors. The studied dependences of the degree of methane conversion and the rate of hydrogen production on the process conditions demonstrated that the degree of methane conversion into hydrogen can reach values close to 100%.

The formed hydrogen, as well as ions and ion-radicals of the hydrogen atom will promote hydrogenation reactions directly in the zone of the main reactions in close proximity to the area of plasma action on the raw material, the excess of reactive particles in the zone of secondary reactions – the hardening zone, will also increase the yield of hydrocarbons with shorter chains filling the open valence bonds formed after the decay of the initial molecules with a high molecular weight, reducing the number of recombination reactions with the formation of compounds with double and triple bonds. Also, by regulating the methane supply, it is possible to obtain the desired selectivity of the process for the final products. The formed ions, ion-radicals of carbon will also participate in the plasma cracking process as reactive particles. This change in the process technology will lead to a reduction in the supply of water vapour or its complete replacement with methane as a plasma-forming gas, which will lead to a reduction in the amount of oxygen-containing compounds in the reaction product, the formation and deposition of soot in the products and on the internal walls of the plant equipment.

Plasma cracking represents a modern technology for converting heavy oil residues and other refractory feedstock (heavy oil residues) into lighter, more valuable products. By harnessing the unique properties of plasma, this method offers superior efficiency, reduced environmental impact, and operational flexibility compared to conventional cracking techniques.

While further research needed to optimise scalability and cost-effectiveness, plasma cracking is poised to play a critical role in the sustainable evolution of hydrocarbon processing. As the energy sector transitions toward greener solutions, this technology provides a viable pathway to maximise resource utilisation while minimising carbon footprints.

Declarations

All authors declare that they have no conflicts of interest.

References

Bartholomew, C.H. and Farrauto, R.J. (2006) *Fundamentals of Industrial Catalytic Processes*, 2nd ed., Wiley, Hoboken, NJ, USA.

Becker, K.H., Kogelschatz, U., Schoenbach, K.H. and Barker, R.J. (2005) *Non-equilibrium Air Plasmas at Atmospheric Pressure*, IOP Publishing, Bristol, UK.

Belichenko, E.E., Belichenko, Y.E. and Grenaderov, A.B. (2008) *Method for Hydrocracking of Heavy Hydrocarbon Fractions and Device for its Implementation*, Russian Patent RU 2319730, March.

Bibikov, M.B. et al. (2007) 'Partial oxidation of kerosene in plume microwave discharge', *High Energy Chem.*, Vol. 41, No. 5, pp.361–365.

Bogaerts, A. and Neyts, E.C. (2018) 'Plasma technology: an emerging technology for energy storage', *ACS Energy Lett.*, Vol. 3, No. 4, pp.1013–1027, DOI: 10.1021/acsenergylett.8b00184.

Bromberg, L., Cohn, D.R., Rabinovich, A., O'Brien, C. and Hochgreb, S. (1998) 'Plasma reforming of methane', *Energy Fuels*, Vol. 12, No. 1, pp.11–18.

Fridman, A. (2008) *Plasma Chemistry*, Cambridge University Press, Cambridge, UK.

Fridman, A. and Kennedy, L.A. (2004) *Plasma Physics and Engineering*, CRC Press, Boca Raton, FL, USA.

Ganieva, G.R., Galeev, I.G., Gismatullin, N.K., Ziganshin, D.I., Takhautdinov, R.S. and Timerkaev, B.A. (2011) 'Decomposition of heavy hydrocarbons in a free electric arc', *Izvestiya Samarskogo Nauchnogo Tsentra Rossiiskoi Akademii Nauk (Proceedings of the Samara Scientific Center of the Russian Academy of Sciences)*, Vol. 13, No. 4, pp.1156–1159, UDC 537.525.

Ganieva, G.R., Timerkaev, B.A., Yakhin, R.G., Yagund, E.M. and Potapova, L.I. (2015) 'Technology of heavy hydrocarbon decomposition by arc discharge', *Innovatsionnaya Nauka (Innovative Science)*, No. 4, p.14, ISSN: 2410-6070.

Gary, J.H., Handwerk, G.E. and Kaiser, M.J. (2007) *Petroleum Refining: Technology and Economics*, 5th ed., CRC Press, Boca Raton, FL, USA.

Holladay, J.D., Hu, J., King, D.L. and Wang, Y. (2009) 'An overview of hydrogen production technologies', *Catal. Today*, Vol. 139, No. 4, pp.244–260.

Holub, M. (2012) 'On the measurement of plasma power in atmospheric pressure DBD plasma reactors', *Int. J. Appl. Electromagn. Mech.*, Vol. 39, Nos. 1–4, pp.81–87.

Jahanmiri, A., Rahimpour, M.R., Shirazi, M.M., Hooshmand, N. and Taghvaei, H. (2012) 'Naphtha cracking through a pulsed DBD plasma reactor: effect of applied voltage, pulse repetition frequency and electrode material', *Chem. Eng. J.*, May, Vol. 191, pp.416–425.

Khademi, M.H., Setoodeh, P., Rahimpour, M.R. and Jahanmiri, A. (2009) 'Optimization of methanol synthesis and cyclohexane dehydrogenation in a thermally coupled reactor using differential evolution (DE) method', *Int. J. Hydrogen Energy*, Vol. 34, No. 16, pp.6930–6944.

Khakimov, A.R., Kirillova, L.B., Pivovarova, N.A. and Belichenko, Y.E. (2012) 'Determination of optimal parameters for plasma-chemical processing of heavy residues from oil mixtures', *Oil, Gas Bus.*, No. 8, pp.62–64.

Khani, M.R. et al. (2011) 'Investigation of cracking by cylindrical dielectric barrier discharge reactor on the n-hexadecane as a model compound', *IEEE Trans. Plasma Sci.*, September, Vol. 39, No. 9, pp.1807–1813.

Khani, M.R. et al. (2014) 'Study on the feasibility of plasma (DBD reactor) cracking of different hydrocarbons (n-hexadecane, lubricating oil, and heavy oil)', *IEEE Trans. Plasma Sci.*, Vol. 42, No. 9, pp.2664–2671, DOI: 10.1109/TPS.2014.2345846.

Kogelschatz, U. (2003) 'Dielectric-barrier discharges: their history, discharge physics, and industrial applications', *Plasma Chem. Plasma Process.*, Vol. 23, No. 1, pp.1–46.

Lemont, F., Marchand, M., Magnin, R. and Mabrouk, M. (2018) 'The Elipse process: an underwater plasma technology for hazardous organic liquid treatment', *Waste Eng. Conference*, Prague, Czech Republic, July [online] https://hal-cea.archives-ouvertes.fr/cea-02339248.

Malik, M.A., Hughes, D., Malik, A., Xiao, S. and Schoenbach, K.H. (2013) 'Study of the production of hydrogen and light hydrocarbons by spark discharges in diesel, kerosene, gasoline, and methane', *Plasma Chem. Plasma Process.*, Vol. 33, No. 1, pp.271–279.

Moulijn, J.A., Makkee, M. and Van Diepen, A.E. (2013) *Chemical Process Technology*, 2nd ed., Wiley, Hoboken, NJ, USA.

Neyts, E.C., Ostrikov, K., Sunkara, M.K. and Bogaerts, A. (2015) 'Plasma catalysis: synergistic effects at the nanoscale', *Chem. Rev.*, December, Vol. 115, No. 24, pp.13408–13446, DOI: 10.1021/acs.chemrev.5b00362.

Nomura, S. et al. (2009) 'Production of hydrogen in a conventional microwave oven', *J. Appl. Phys.*, October, Vol. 106, No. 7, p.073306.

Pierce, R.G., Padron-Wells, G. and Goeckner, M.J. (2009) 'Gas-phase chemistry of pulsed n-hexane discharge', *Plasma Chem. Plasma Process.*, Vol. 29, No. 1, pp.1–11.

Prieto, G., Prieto, O., Gay, C.R., Mizuno, A., Takashima, K. and Yamamoto, T. (2008) 'Nonthermal plasma reactors and plasma chemistry', *Int. J. Environ. Waste Manag.*, Vol. 2, No. 4, pp.349–398.

Purm.ru, *Metal Plasma Cutting Machine PURM-400VA (with BAO)* [online] https://purm.ru/product/apparat-plazmennoj-rezki-metalla-purm-400va/ (accessed 1 September 2025).

Riyanto, T. et al. (2020) 'Plasma-assisted catalytic cracking as an advanced process for vegetable oils conversion to biofuels: a mini review', *Ind. Eng. Chem. Res.*, Vol. 59, No. 40, pp.17632–17652, DOI: 10.1021/acs.iecr.0c03253.

Ryabov, V.D. (2004) *Chemistry of Oil and Gas*, Tekhnika, Moscow, Russia.

Sadeghbeigi, R. (2012) *Fluid Catalytic Cracking Handbook: An Expert Guide to the Practical Operation, Design, and Optimization of FCC Units*, Elsevier, Amsterdam, The Netherlands.

Slovetskii, D.I. (2006) 'Plasma-chemical processes in petroleum chemistry (review)', *Pet. Chem.*, Vol. 46, No. 5, pp.295–304.

Speight, J.G. (2010) *The Refinery of the Future*, William Andrew, Norwich, NY, USA.

Suttikul, T., Tongurai, C., Sekiguchi, H. and Chavadej, S. (2012) 'Ethylene epoxidation in cylindrical dielectric barrier discharge: Effects of separate ethylene/oxygen feed', *Plasma Chem. Plasma Process.*, Vol. 32, No. 6, pp.1169–1188.

Taghvaei, H., Jahanmiri, A., Rahimpour, M.R., Shirazi, M. and Hooshmand, N. (2013) 'Hydrogen production through plasma cracking of hydrocarbons: effect of carrier gas and hydrocarbon type', *Chem. Eng. J.*, January, Vol. 226, pp.384–392.

Vodopyanov, A.V. et al. (2022) 'Methane plasmolysis using a high-frequency plasmatron', *Tech. Phys. Lett.*, October, Vol. 48, No. 23, pp.34–37.

Yarullin, M.R. (2000) *Development of a Technology for Producing Unsaturated Hydrocarbons by Plasma-chemical Methods*, Cand. Tech. Sci. Diss.: 02.00.13, 151pp., Kazan.

Zalyaletdinov, F.D. (2011) *Decomposition of Heavy Hydrocarbons into Light Fractions Using Electric Arc Plasma*, Cand. Tech. Sci. Diss.: 01.02.05, 117pp., Kazan.